This article was downloaded by:
On: *22 January 2011*
Access details: *Access Details: Free Access*
Publisher *Taylor & Francis*
Informa Ltd Registered in England and Wales Registered Number: 1072954 Registered office: Mortimer House, 37-41 Mortimer Street, London W1T 3JH, UK

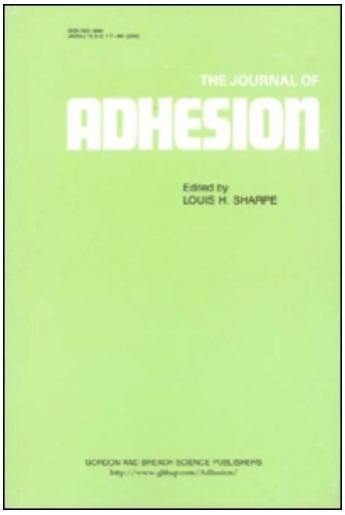

The Journal of Adhesion
Publication details, including instructions for authors and subscription information:
http://www.informaworld.com/smpp/title~content=t713453635

A Comparative Hydrogen Bonding and Fiber Interface Study of Epoxy and Cyanate Resins

A. W. Snow[a]; J. P. Armistead[a]
[a] Naval Research Laboratory, Washington D.C., USA

To cite this Article Snow, A. W. and Armistead, J. P.(1995) 'A Comparative Hydrogen Bonding and Fiber Interface Study of Epoxy and Cyanate Resins', The Journal of Adhesion, 52: 1, 223 — 250
To link to this Article: DOI: 10.1080/00218469508015195
URL: http://dx.doi.org/10.1080/00218469508015195

PLEASE SCROLL DOWN FOR ARTICLE

Full terms and conditions of use: http://www.informaworld.com/terms-and-conditions-of-access.pdf

This article may be used for research, teaching and private study purposes. Any substantial or systematic reproduction, re-distribution, re-selling, loan or sub-licensing, systematic supply or distribution in any form to anyone is expressly forbidden.

The publisher does not give any warranty express or implied or make any representation that the contents will be complete or accurate or up to date. The accuracy of any instructions, formulae and drug doses should be independently verified with primary sources. The publisher shall not be liable for any loss, actions, claims, proceedings, demand or costs or damages whatsoever or howsoever caused arising directly or indirectly in connection with or arising out of the use of this material.

J. Adhesion, 1995, Vol. 52, pp. 223–250
Reprints available directly from the publisher
Photocopying permitted by license only

© 1995 OPA (Overseas Publishers Association)
Amsterdam B.V. Published under license by
Gordon and Breach Science Publishers SA
Printed in Malaysia

A Comparative Hydrogen Bonding and Fiber Interface Study of Epoxy and Cyanate Resins

A. W. SNOW and J. P. ARMISTEAD

Naval Research Laboratory, Washington, D.C. 20375, USA

(Received May 10, 1994; in final form January 5, 1995)

A spectroscopic method based on model compounds for measuring and ranking thermoset resin hydrogen bond acceptor and donor strengths is demonstrated. This method involves measurements of complex formation constants between polyfunctional resin model compounds and monofunctional probe compounds. For the epoxy (m-phenylenediamine/bisphenol A diglycidyl ether and 1,3-diaminocyclohexane /bisphenol A diglycidyl ether) and cyanate (bisphenol A dicyanate) resins of this study, the ranking of hydrogen bond basicity is aliphatic amine-epoxy > cyanate > aromatic amine-epoxy, and the ranking of hydrogen bond acidity is aromatic amine-epoxy > aliphatic amine-epoxy ≫ cyanate. For the amine-epoxy resin model compounds, intramolecular interactions between the amine and hydroxyl groups reduce the hydrogen bond acceptor strength and enhance the hydrogen bond donor strength relative to expectations for these individual functional groups acting independently. Measurements of the hydrogen bond basicity of the resin monomer model compounds are also reported. Results of single fiber fragmentation tests of an AS4 carbon fiber with the MPDA-epoxy, DACH-epoxy and cyanate resins are indicative of good adhesion and are in a ranking order parallel to that of the hydrogen bond basicity. There is minimal mechanical property variation among these resins, and a hydrogen bonding mechanism is proposed for the correlation of fiber-resin interfacial shear strength and resin hydrogen bond basicity.

KEY WORDS: hydrogen bonded interactions; thermoset resin model compounds; hydrogen bonded complexes; carbon fiber/amine-epoxy composite; carbon fiber/cyanate composite; fiber-matrix interface.

Downloaded At: 12:28 22 January 2011

INTRODUCTION

Hydrogen bonded interactions are important contributors to cohesive and adhesive properties of thermoset polymers. These effects relate directly to individual molecular functional group structures such as hydroxyl, ether, amine, etc. As such, when studied individually on low molecular weight compounds, the hydrogen bond acceptor and donor strengths of each functional group can be measured and quantitatively compared. A hydrogen bond donor is a molecule (or functional group) that donates a proton in the hydrogen bonded complex. A hydrogen bond acceptor is a molecule that provides a bonding site (*e.g.* a nonbonded electron pair) to accept the proton in the hydrogen bonded complex.

For the situation of a fluid thermosetting monomer being cured around a fiber, hydrogen bonded interactions at the interface have effects on the resin curing reaction as well as on adhesive interactions between the cured resin and the fiber surface. For example, an epoxy-amine curing reaction has been shown to be accelerated at a carbon

interface by hydrogen bonded interactions,[1] and carbon fiber-epoxy matrix adhesion has been correlated with acid-base interactions determined from inverse gas chromatography measurements.[2] These examples correlate macroscopic measurements (*i.e.* DSC and inverse GC) with presumed microscopic effects (*i.e.* hydrogen bonding and acid-base interactions). The approach of this work is to measure directly the strength of hydrogen bonded interactions at functional groups on monomer and cured resin structures with the objective of correlating the strength of the hydrogen bonding with macroscopic adhesive behavior. For cured thermoset resin structures, hydrogen bond measurements are complicated by intramolecular functional group interactions and a postgelation insolubility. By selecting appropriate model compounds for these thermoset resin structures, such measurements can be made. Interpreting these measurements is complicated by the polyfunctional character of the model compounds, and caution should be exercised in the extrapolation from model compound to resin structure. While this complication makes a fundamental understanding of the hydrogen bonded interaction measurement difficult, it is not detrimental to utilizing such measurements as a tool for quantitatively ranking resins as to this interaction. Such a characterization parameter could be of particular value in the design and selection of thermosets for various properties and applications.

This paper describes our efforts at characterizing the hydrogen bond acceptor and donor strengths for monomers and model compounds of three thermoset resin systems and at correlating these hydrogen bond parameters with a resin-to-carbon-fiber interface adhesion measurement.

Downloaded At: 12:28 22 January 2011

BACKGROUND

The idea of using a probe molecule to measure hydrogen bonded interactions may be traced back to 1938 when Gordy utilized chloroform to study hydrogen bonding with acetone, ethyl acetate, dioxane and diethyl ether.[3] To quantify the strength of a hydrogen bonding interaction an energy parameter is measured when a donor and acceptor form a hydrogen bond complex. This energy parameter may be a directly-measured spectroscopic shift caused by the complex formation (*e.g.* frequency shift in the infrared O-H absorption) or a thermodynamic quantity (*i.e.* complex formation constant and hydrogen bond enthalpy determined therefrom) usually determined from concentration-dependent spectroscopic measurements. Various spectroscopies (IR, Raman, NMR, and electronic) display these frequency shifts and have proved essential for measuring the hydrogen bonding interactions.[4] A relationship between the energy of the hydrogen bond and the observed spectroscopic frequency shift was postulated many years ago,[5] and linear relationships were later reported,[6,7] Drawing on the concepts of donor/acceptor (acid/base) molecular interactions[8] or linear complexation free energy relationships,[9] these relationships have been developed into a variety of quantitative methods for characterizing the hydrogen bonding donor-acceptor properties of molecular substances which include solvents,[9] solutes,[10] solids[11] and surfaces.[2,12] In the case of discrete, nonassociated molecular species, the most common procedure for evaluating relative hydrogen bonding acceptor strengths involves either the calorimetric or spectroscopic characterization of their interaction with a reference

donor compound (or *vice versa* for the evaluation of relative hydrogen bonding donor strength) using dilute solutions of the species in question in an inert (*i.e.*, nonhydrogen bonding) solvent environment. For our evaluation of hydrogen bond acceptor strengths we have chosen the method of Gurka and Taft.[13] This involves measurement of the relative ^{19}F NMR chemical shift induced by hydrogen bond complex formation between the species of interest and the reference donor compound, *p*-fluorophenol, in dilute carbon tetrachloride solution. Likewise, for our evaluation of relative hydrogen bond donor strength we have chosen the method of Frange, *et al.*[14] This involves measurement of the relative absorption intensity of the $n \rightarrow \pi^*$ electronic transition induced by hydrogen bond complex formation between the species of interest and the reference acceptor compound, pyridine N-oxide, in dilute cyclohexane solution.

Efforts in our laboratory have focused on physical and chemical factors that contribute to load transfer between thermoset resins and carbon fibers. In previously reported work, involving epoxy and cyanate resins and high strength and high modulus carbon fibers, the effects of resin physical properties on the single fiber fragmentation load transfer test were studied.[15] These properties included critical surface energy for wetting, cure shrinkage, thermal shrinkage and mechanical modulus and strength. Chemical interactions across the interface were not considered. From a consideration of the resins' structures and the nature of the carbon fiber surface, hydrogen bonding appears to be a major contributor to interfacial adhesion.

The epoxy and cyanate resin structures are illustrated in Figure 1. The various sites for hydrogen bonding are hydroxyl, amine and ether functional groups of the amine-epoxy resins and are triazine and ether functional groups of the cyanate resin. For the purpose of strongly varying the amine basicity with minimal structural variation, the amine-epoxy prepared from the saturated analog of m-phenylenediamine, 1,3-diaminocyclohexane, was included. Aliphatic amine basicity is a factor of 10^6 greater than aromatic amine basicity. The hydrogen bond acceptor and donor strength measure-

Downloaded At: 12:28 22 January 2011

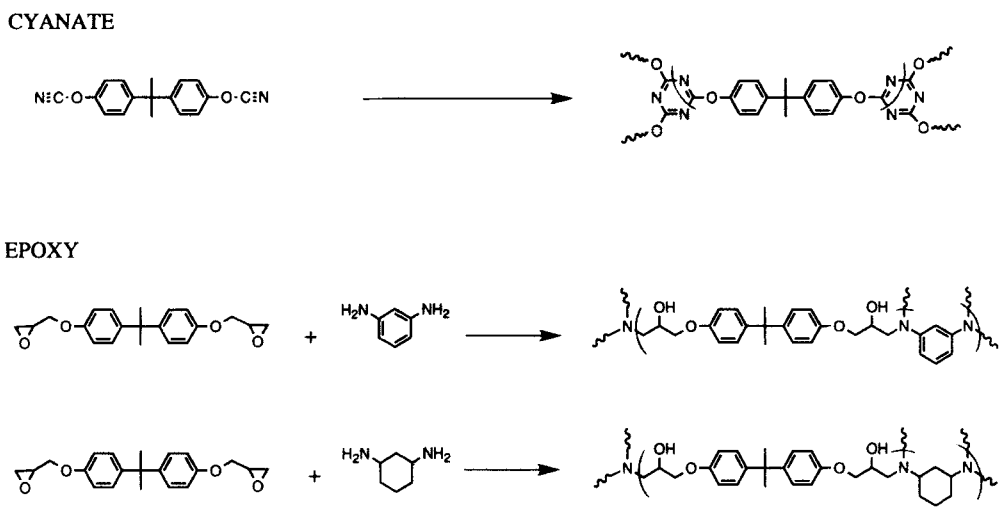

FIGURE 1 Structures and reactions of cyanate and epoxy monomers and cured resins.

ments require a soluble system so that the complex formation constant with the probe molecule can be determined. For this purpose, thermoset resin model compounds are used in place of the resin. The model compounds for the resins of Figure 1 are illustrated in Figure 2.

The carbon fiber selected for this work is the Hercules AS4 fiber. This is an unsized, surface-treated, high-strength carbon fiber. Its surface composition by XPS analysis was previously reported as 82.2% carbon, 14.7% oxygen and 3.1% nitrogen.[16] This result is typical for AS4 fibers as reflected by a range of collected results of this analysis on this commercial fiber.[17] Commercial carbon fibers generally receive proprietary oxidative surface treatments to promote adhesion to resins. The oxidized carbon fiber surface has been characterized by spectroscopic,[18-20] wet chemical [18-20] and inverse gas chromatographic[2] techniques as acidic with an indicated presence of phenol, carboxylic acid and quinoid groups.[17-22] As such, hydrogen bonded interactions at the carbon fiber surface should be stronger with resins of greater basicity. If chemical interactions are the determining factor in the strength of the interface, then a correlation should exist between the interfacial shear strength measurement and the resin hydrogen bond acceptor strength.

Downloaded At: 12:28 22 January 2011

EXPERIMENTAL

All reagents and solvents were of reagent grade quality, purchased commercially and used without further purification unless otherwise noted. Spectroscopic data were obtained from the following associated instruments: UV/Perkin-Elmer Lambda 5, IR/Perkin-Elmer Model 1800 FTIR, and ^{1}H and ^{19}F NMR/Varian EM390 (90 MHz) with TMS and $CFCl_3$ references, respectively. Gas chromatography measurements were obtained by using a Varian GC Model 3700 equipped with a Hewlett-Packard

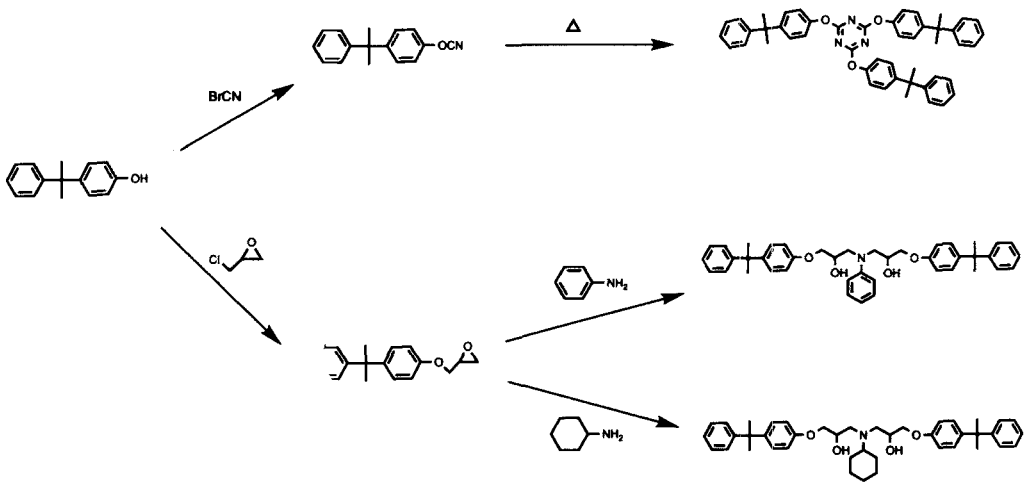

FIGURE 2 Structures and reactions of cyanate and epoxy monofunctional monomers and resin model compounds.

Model 3390A integrator. Differential scanning calorimetry (DSC) measurements of T_g were made with a Perkin-Elmer DSC-7. Melting points are uncorrected. Elemental analyses were performed by Schwarzkopf Microanalytical Laboratory, Woodside, NY, USA.

Synthesis of Model Compounds

4-(2-(2-Phenylpropyl)) Phenyl-2', 3'-epoxypropyl ether, (cumylphenyl glycidyl ether, CPGE). To a 3-neck 100 ml flask fitted with a thermometer, dropping funnel and nitrogen inlet, were added 8.48 g (0.020 mol) cumylphenol and 37.0 g (0.20 mol) epichlorohydrin (freshly distilled). A solution of 1.60 g (0.20 mol) NaOH in 6 g water was added, and the mixture was refluxed at 95–105°C with stirring for 9 hr. The reaction was worked up by separating the aqueous salt phase, and extracting the epichlorohydrin phase with 40 ml water and drying over Na_2SO_4. The epichlorohydrin-water azeotrope was distilled (80–90°C/760 mm) followed by distillation of the excess epichlorohydrin (120°C/760 mm). The crude product was then distilled (160–170°C/0.5 mm) to yield 8.65 g. GC analysis indicated two easily resolved components, and IR spectra indicated presence of a hydroxyl (3450 cm^{-1}) impurity. This impurity was removed by passing the product through an alumina column (Woelm, neutral, activity 1) with methylene chloride elution. Analyses: IR, see Figure 3; ^1H NMR ($CDCl_3$) δ1.65 (S, 6H), δ2.8 (m, 2H), δ3.3 (m, 1H), δ4.05 (m, 2H), δ6.8–7.3 (m, 9H); m/e 268 (P).

N,N'-Bis-[3-(4-(2-(2-phenylpropyl))phenoxy)-2-hydroxypropyl]aniline (2:1 cumylphenyl glycidyl ether-aniline adduct, AREP). To a 10 × 75 mm tube fitted with a small stirring bar and nitrogen inlet were added 0.248 g (0.925 mmol) CPGE and 0.0449 g (0.483 mmol) aniline (freshly distilled). This mixture was heated with stirring at 75°C for 2 hr and at 125°C for 4 hr. After cooling, the product was dissolved in chloroform and chromatographed on an alumina column (Woelm, neutral, activity 1) with 5% methanol/chloroform elution. IR and GC detected no unreacted aniline or CPGE. The product was vacuum dried at 60°C and crystallized on standing. Yield 0.24 g. Analysis: IR, see Figure 3; ^1H NMR (CCl_4) δ1.60 (s, 6H), δ3.15 (m, 1H), δ3.5 (m, 1H), δ3.8 (m, 2H), δ4.15 (m, 1H), δ6.5–7.2 (m, 9H); elemental, calculated for $C_{42}H_{47}O_4N$: C, 80.13%; H, 7.47%; N, 2.22%. Found: C, 80.02%; H, 7.68%; N, 2.10%.

N,N'-Bis-[3-(4-(2-(2-phenylpropyl))phenoxy)-2-hydroxypropyl]amino-cyclohexane, (2:1 cumylphenyl glycidyl ether-aminocyclohexane adduct, ALEP). To a 10 × 75 mm tube fitted with a small stirring bar and nitrogen inlet were added 0.257 g (0.958 mmol) CPGE and 0.0475 g (0.449 mmol) cyclohexylamine (freshly distilled). This mixture was heated with stirring at 75°C for 2 hr and at 125°C for 2 hr. After cooling, the product was a viscous gum. It was dissolved in chloroform and chromatographed on an alumina column (Woelm, neutral, activity 1) with 5% methanol/chloroform elution. IR and GC detected no unreacted amine or CPGE. The product was vacuum dried at 55°C. It did not crystalize on standing but remained a soft gum. Yield 0.21 g. Analysis:

Downloaded At: 12:28 22 January 2011

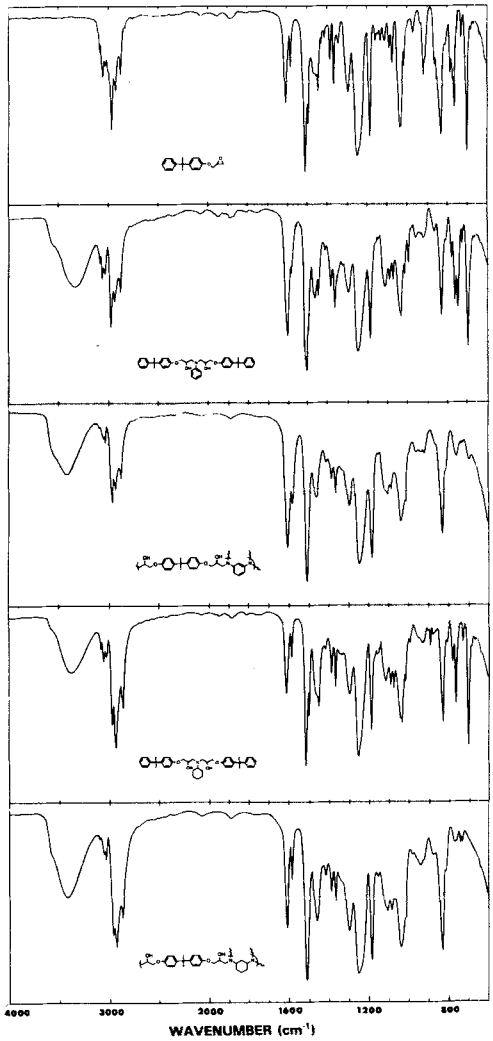

FIGURE 3 IR spectra of aromatic-amine epoxy and aliphatic amine epoxy cured resins and model compounds.

IR, see Figure 3; elemental, calculated for $C_{42}H_{53}O_4N$: C, 79.37%; H, 8.35%; N, 2.20%. Found: C, 78.99%; H, 8.44%; N, 2.07%.

2-Phenyl-2-(4-cyanatophenyl) propane, (cumylphenyl cyanate, CPCY). This compound was prepared from reaction of cumylphenol with cyanogen bromide as previously reported.[23]

Tris (4-cumylphenoxy)-1,3,5-triazine, (cumylphenoxytriazine, CPTZ). This compound was prepared by trimerization of CPCY as previously reported.[23]

Downloaded At: 12:28 22 January 2011

β-Scale Hydrogen Bond Acceptor Strength Measurements

The procedure for measuring the hydrogen bonded complex formation constant and limiting spectral shift for a model compound with *p*-fluorophenol closely conformed with that reported by Gurka and Taft.[13] The carbon tetrachloride solvent was distilled from calcium hydride. The *p*-fluorophenol was sublimed, and the *p*-fluoroanisole was distilled. A 0.020 M stock solution was immediately prepared by dissolving 0.0556 g *p*-fluorophenol and 0.0644 g *p*-fluoroanisole in 25 ml carbon tetrachloride. The pure components and stock solution were transferred to Teflon septum capped vials and stored in a nitrogen-filled desiccator. For the measurement, the NMR spectrometer was set to record the ^{19}F NMR spectrum of the *p*-fluorophenol *p*-fluoroanisole combination on a 5 ppm scan at a high sensitivity setting. The probe temperature was 24°C. A series of chemical shift measurements was initiated by pipetting 2.00 ml of the stock solution into a 3.5 ml vial. To this was added an accurate milligram (or submilligram) quantity of model compound. After dissolution, approximately 0.5 ml was transferred to a 5 mm NMR cell and the consequent shift of the *p*-fluorophenol relative to the *p*-fluoroanisole was measured. The contents of the cell were returned to the vial for successive additions of milligram quantities of model compound and the subsequent chemical shift measurement repeated.

For data workup, analytical molar concentrations of model compound were calculated assuming additivity of volumes. The complex hydrogen bonded formation constants and limiting chemical shifts were determined by a computer iteration best fit of the data to a two-component, one-step equilibrium model described in the text.

Downloaded At: 12:28 22 January 2011

α-Scale Hydrogen Bond Donor Strength Measurements

The procedure for measuring the hydrogen bonded complex formation constant for a model compound with pyridine N-oxide hydrogen bond acceptor probe compound was adapted from that reported by Frange *et al.*[14] The slightly-colored commercial pyridine oxide was recrystallized from cyclohexane. This occurred with some difficulty as the saturated cyclohexane solution became cloudy on cooling, then coagulated into crystals or settled as an oily residue on standing overnight. The recrystallized pyridine oxide was then sublimed under vacuum at 60–70°C. The cyclohexane solvent was distilled from lithium aluminum hydride. A first analytical stock solution (9.62×10^{-4} M) was prepared by dissolving 0.0183 g pyridine oxide in 200 ml cyclohexane. A working stock solution (1.92×10^{-4} M) was then prepared by diluting 40 ml of the first stock solution to a 200 ml volume. For the 10 cm path length cells used, this concentration has an absorbance of approximately 1 at the 337.4 nm maximum. The pure components and stock solutions were also transferred to Teflon septum capped vials and stored in a nitrogen-filled desiccator. For the measurement, the UV spectrometer was set to record absorbance on a 0 to 1 scale for a 370 to 320 nm scan. The measurement temperature was 24°C. A series of absorbance measurements was initiated by filling the 10 cm cell with a measured quantity (*ca.* 23 g) of the 1.92×10^{-4} M stock solution, and the absorbencies at the 337.4 nm maximum and at 370 nm were measured. The 370 nm measurement is used to correct for baseline shift that may occur on removal and replacement of the cell between measurements. Dissolution of

the milligram quantities of model compound in the stock solution was accomplished in the 10 cm cell itself. The cell has two cylindrical ports which may be tightly capped with Teflon stoppers. The model compounds were introduced to the cell with a 10 μl microliter syringe through a port and thoroughly mixed by inverting the tightly capped cell and allowing gentle turbulence of several inversions to accomplish the mixing action. Liquid model compounds were transferred directly by the syringe. Solid model compounds were prepared as 10 to 50 weight percent solutions in cyclohexane for the syringe transfer. One exception was CPTZ whose solubility required that carbon tetrachloride be used in place of cyclohexane for this concentrated solution. The 10 μl microliter syringe was calibrated gravimetrically by several injections into a septum-capped vial before each series of measurements.

For data workup, volumes of mixing are assumed to be additive. The concentration unit used to determine equilibrium constants is the mole fraction rather than molarity. This occurs because there are multiple equilibria involved with a single measurement, and the mole fraction unit's interdependency for the individual components allows the equilibrium expressions to be combined to a workable form. However, for the three-step equilibrium model the data workup is still very complex and requires a double computer iteration to obtain the equilibrium constants for the best fit of the data to a three- step equilibrium model. We find that the procedure of Reference 14a does work and strongly recommend that a data set from the supplementary material of Reference 14b be obtained to insure that the computer routine is operating correctly. The equilibrium constants obtained from this workup are in units of mole fraction and need to be converted to units of molarity for calculation of the α-scale hydrogen bond donor strength. For dilute solutions, as in the present work, the following conversion is useful:

$$K_M = \frac{M_s}{1000\rho_s} K_X$$

where K_M is the molarity equilibrium constant, K_X is the mole fraction equilibrium constant, M_s is the solvent molecular weight and ρ_s is the solvent density.

Downloaded At: 12:28 22 January 2011

Resin Cure Procedures

m-Phenylenediamine-bisphenol A diglycidyl ether (MPDA-epoxy). The epoxy resin, diglycidyl ether of bisphenol A (Epon 828, Shell, epoxy equivalent weight 180 g), was obtained from the manufacturer and cured with *m*-phenylenediamine (MPDA). The commercial MPDA was strongly colored and, therefore, was purified by distillation (170°C/6 mm). The bisphenol A epoxy *m*-phenylenediamine resin was prepared by degassing the epoxy under vacuum (20 mm) at 75°C for 5 min, adding 14.5 phr m-phenylenediamine, degassing at 75°C/40 mm until the amine melted and dissolved (about 5 min) and transferring to a preheated mold. The MPDA-epoxy cure schedule was 75°C/2 hr and postcure at 125°C/2 hr.

1,3-Diaminocyclohexane-bisphenol A diglycidyl ether (DACH-epoxy). The diglycidyl ether of bisphenol A (see above) was cured with a stoichiometric quantity of 1,3-diaminocyclohexane (DACH). The commercial DACH had a trace of amber color and was purified by distillation. The bisphenol A epoxy 1,3-diaminocyclohexane resin was

prepared by degassing the epoxy under vacuum (20 mm) at 70°C for 5 min, adding 15.3 phr 1,3-diaminocyclohexane, degassing at 50°C/40 mm for 3 min to yield a uniform colorless solution and transferring to a preheated mold. The DACH-epoxy cure schedule was 50°C/1 hr, 65°C/2 hr, 100°C/1 hr and 125°C/2 hr.

Bisphenol A dicyanate. The dicyanate of bisphenol A monomer (AroCy B-10, Rhône-Poulenc (currently available from Ciba)) was cured with a copper acetylacetonate-nonylphenol catalyst solution.[24] This cyanate resin was cured by degassing the molten bisphenol A dicyanate monomer under vacuum at 95°C for 5 min, adding 3.1 phr of catalyst solution (0.17 g copper in 4.80 g nonylphenol), degassing under vacuum at 95°C for 5 min and transferring to a preheated mold. The cure schedule was 100°C/2 hr, 180/4 hr and 225°C/2 hr.

Thermal Quenching and Tensile Testing of Resin

Using the above cure cycles, resin specimens were prepared as $\frac{1}{8}$-inch (3.18 mm) thick panels in aluminum molds coated with a dry fluorocarbon release agent. Unless otherwise specified, all heating and cooling rates were 2°C/min with a thermocouple mounted to the mold surface providing feedback temperature control to the heating controls of a Blue M forced draft oven. The epoxy panels were subsequently reheated in a supporting mold to 20°C above the T_g for 30 min and subjected to either a slow cooled or a quenched thermal treatment. Teflon liners in the mold prevent a severe thermal gradient on the resin surface during quenching. The quench treatment involved immersion of the mold in a 0°C ice bath. The cooling rate for this quench procedure has been measured at 40°C/min.[25] The slow cooled treatment was programmed at 2°C/min for the MPDA-epoxy and 0.5°C/min for the DACH-epoxy resins. For the cyanate resin specimens, attempted thermal treatment at 20°C above the 280°C T_g resulted in a darkening of the specimen and premature failure in the grip during the tensile test. The procedure was revised so that freshly-cured cyanate resin panels were reheated to 255°C in a supporting mold without a Teflon liner and then either slow cooled (2°C/min) or quenched (into 20°C water bath). ASTM E8 dogbone-shaped tensile test specimens were machined from the treated resin panels using a Tensilkut router device with carbide bits. Sharp edges were sanded with #600 abrasive paper prior to testing. Quenched samples were tested between 6 to 8 hr after the quench treatment. Stress-strain measurements were made using an Instron (Model 4206) with a 1000 lb (455 kg) load cell, wedge grips and a clamp-on extensometer. The initial grip separation was 46 mm, and the cross head speed was 1.25 mm/min.

Single Fiber Fragmentation Tests

Test specimens were prepared by positioning appropriately-spaced single carbon fibers in the resin panel mold prior to transfer and curing of the resin. The dogbone-shaped tensile test specimens with the fiber centered at the axis were machined as described above. Before testing, the specimens were subjected to a thermal quench as also described above. The specimens were slowly strained on the stage of a Zeiss UEM polarizing

Downloaded At: 12:28 22 January 2011

microscope with a hand-operated, screw-type straining apparatus until fiber fragmentation ceased. The lengths of the fiber fragments along the dogbone axis were measured using a viewing tube and digitizing pad. The diameter ($7.1 \pm .3\ \mu m$) and tensile strength as a function of gage length for this AS4 fiber have been previously reported.[15]

RESULTS AND DISCUSSION

Synthesis of Model Compounds

The model compounds for the resins in Figure 1 are synthesized from the monofunctional analogues of the resin monomers. The schemes for these syntheses are presented in Figure 2. Cumylphenol is the common starting reagent and is readily reacted with epichlorohydrin or cyanogen bromide to yield the corresponding epoxy and cyanate resin monomers.

For the corresponding aromatic amine-epoxy and aliphatic amine-epoxy resin model compounds, the cumylphenyl glycidyl ether is reacted in 2:1 stoichiometry with aniline and with cyclohexylamine, respectively. These model compounds are purified by alumina column chromatography, and characterization data are presented in the Experimental Section. These compounds have two asymmetric centers and are mixed stereoisomers. A mechanical separation of similar stereoisomers based on crystalline form has been reported and analyzed by ^1H NMR for a *t*-butylphenyl glycidyl ether aniline adduct.[26] Similar ^1H NMR features are detected for this cumylphenyl system, but its crystallization behaviour is such that no analogous separation could be made. For illustration of similarity of the model compounds with their respective resins, the IR spectra are presented in Figure 3.

The cyanate resin model compound is prepared by trimerization of the cumylphenyl cyanate monomer with heat in the presence of a trace of aluminum trichloride.[23] This model compound is readily purified by recrystalization. Its IR spectrum along with that of the corresponding cyanate resin have been previously reported.[23]

β-Scale Hydrogen Bond Acceptor Measurements

The hydrogen bond acceptor strength of these model compounds is measured by complex formation with a reference hydrogen bond donor compound. These measurements are made in dilute solution with a nonhydrogen bonding solvent. The ^{19}F NMR chemical shift method using *p*-fluorophenol and *p*-fluoroanisole in carbon tetrachloride solution was selected.[13] The equilibrium is illustrated below.

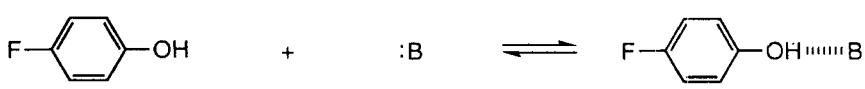

A B AB

$$K_{HB} \doteq \frac{[AB]}{[A]\,[B]} = \frac{(\delta/\Delta)\,A^0}{A^0\,[1 - \delta/\Delta]\,[B^0 - (\delta/\Delta)\,A^0]} \qquad (1)$$

Downloaded At: 12:28 22 January 2011

The chemical shift of the *p*-fluorophenol fluorine nucleus is modulated by electron density shifts caused by hydrogen bonding of the phenol (A) with an added base (B). Initially, the *p*-fluorophenol and *p*-fluoroanisole ^{19}F NMR signals have coincident chemical shifts. Incremental additions of the hydrogen bond acceptor compound (*i.e.* resin model compound or monomer) drives the equilibrium to the right, and an ^{19}F chemical shift displacement (δ) of the *p*-fluorophenol relative to the *p*-fluoroanisole results. When a large excess of the hydrogen bond acceptor compound has been added and the equilibrium is shifted far to the right, this *p*-fluorophenol ^{19}F chemical shift displacement approaches a limiting chemical shift (Δ) characteristic of the hydrogen bonded complex. A series of spectra illustrating this measurement is presented in Figure 4. Since the equilibrium is rapid on the NMR time scale, the observed *p*-fluorophenol ^{19}F chemical shift displacements relative to the limiting chemical shift is an average of the complexed and uncomplexed *p*-fluorophenol and is proportional to the degree of shift of the equilibrium. The quantity of hydrogen bond complex formed, $[AB]$, is then given by $(\delta/\Delta)A^\circ$, and the quantities of uncomplexed phenol and base are given by $[1-(\delta/\Delta)]A^\circ$ and $[B^\circ-(\delta/\Delta)A^\circ]$ where A° and B° are the analytical

Downloaded At: 12:28 22 January 2011

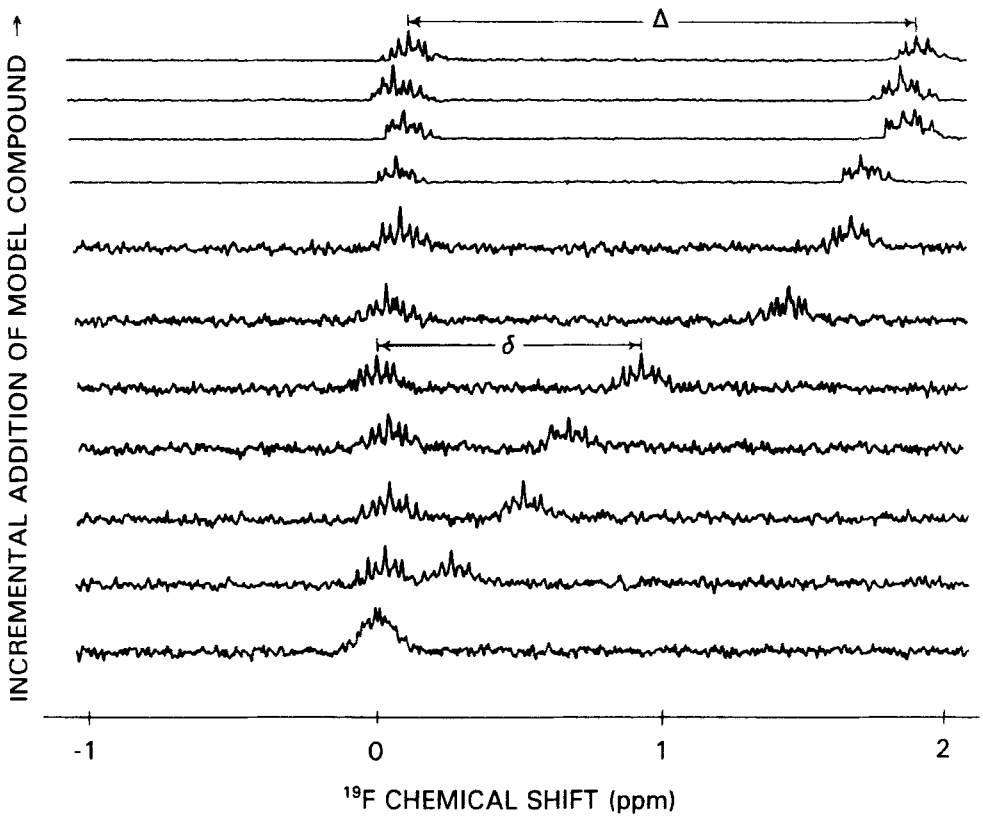

FIGURE 4 ^{19}F NMR spectra of *p*-fluorophenol (0.020 M in CCl_4) relative to *p*-fluoroanisole illustrating increasing chemical shift caused by hydrogen bond complex formation with incremental additions of model compound.

quantities of phenol and base. The complex formation constant (K_{HB}) is determined by the chemical shift displacement dependence on the concentration of added hydrogen bond acceptor compound. The strength of the hydrogen bond is related to both K_{HB} and Δ.

In practice, several data sets of the fluorophenol chemical shift (relative to fluoroanisole) and concentration of added hydrogen bond acceptor compound are collected. The values of K_{HB} and Δ are determined by iteration according to equation (1) to obtain a plot which best fits the experimental data. These data and plots are presented in Figure 5. The magnitude of K_{HB} is determined by the slope of the curve, and that of Δ is determined by the maximum value of δ approached by the curve. It is immediately obvious that the order of hydrogen bond acceptor strength of the resin model compounds is aliphatic amine-epoxy > cyanate > aromatic amine-epoxy. A β-scale of hydrogen bond acceptor strengths has been defined which is independent of the hydrogen bond donor reference compound and is normalized to a scale of 0 to 1[9]. The respective β-scale correlation equations for K_{HB} and Δ values of the fluorophenol reference compound are[9]:

$$\beta_\Delta = \frac{^{19}\text{F NMR } \Delta}{(2.80)(1.356)} \qquad \beta_K = \frac{pK_{HB} + 1.00}{(2.80)(1.571)}$$

Both β-scale values for the three resin model compounds are entered in Table I. One value serves to check the other, and the agreement is relatively good.

Downloaded At: 12:28 22 January 2011

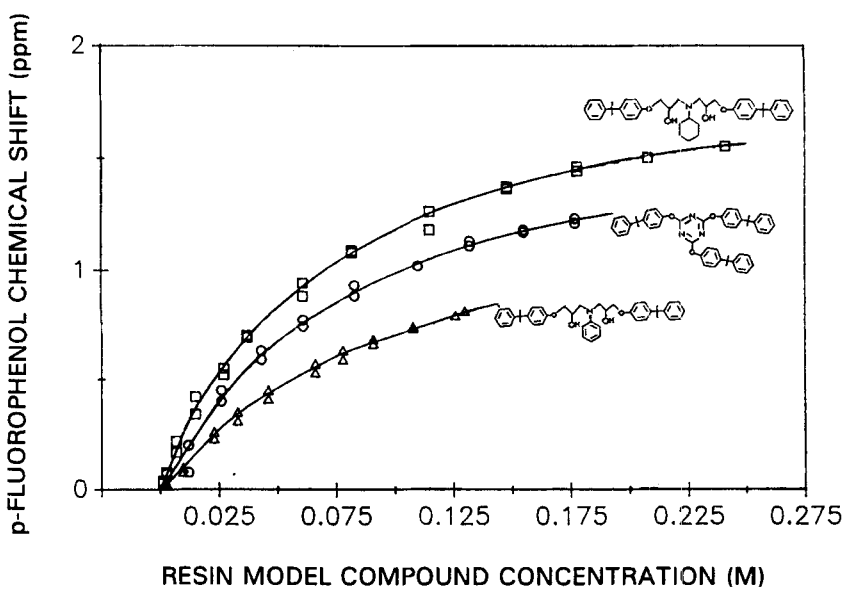

FIGURE 5 Resin model compound—p-fluorophenol hydrogen bond complexation data fit to equation (1) for determination of Δ and K_{HB} and calculation of β_Δ and β_K.

TABLE I
β_Δ and β_K Hydrogen Bond Acceptor Strength Measurements on Epoxy and Cyanate Model Systems.

AROMATIC AMINE EPOXY	β_Δ	β_K
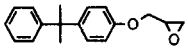	.36	.39
	.36	.38
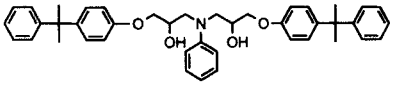	.43	.43
ALIPHATIC AMINE EPOXY		
	.68	.74
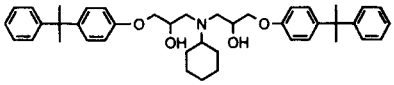	.50	.52
CYANATE		
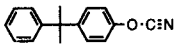	.41	.41
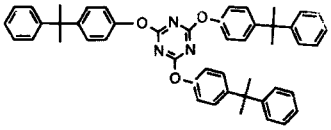	.47	.48

In the process of making these measurements on the resin model compounds it became of interest to determine whether the precursor cyanate, amine and epoxy monomers might differ appreciably in hydrogen bond basicity. If such is the case, a selective adsorption of the stronger hydrogen bonding monomer onto an acidic surface may occur. This can result in a local mismatch of the amine-epoxy stoichiometry with a consequent alteration of the mechanical properties of the resin at the interface. Analogous hydrogen bond basicity measurements were conducted on the corresponding monofunctional amine, epoxy and cyanate monomers (Figure 6), and the β-scale values are also entered in Table I.

Downloaded At: 12:28 22 January 2011

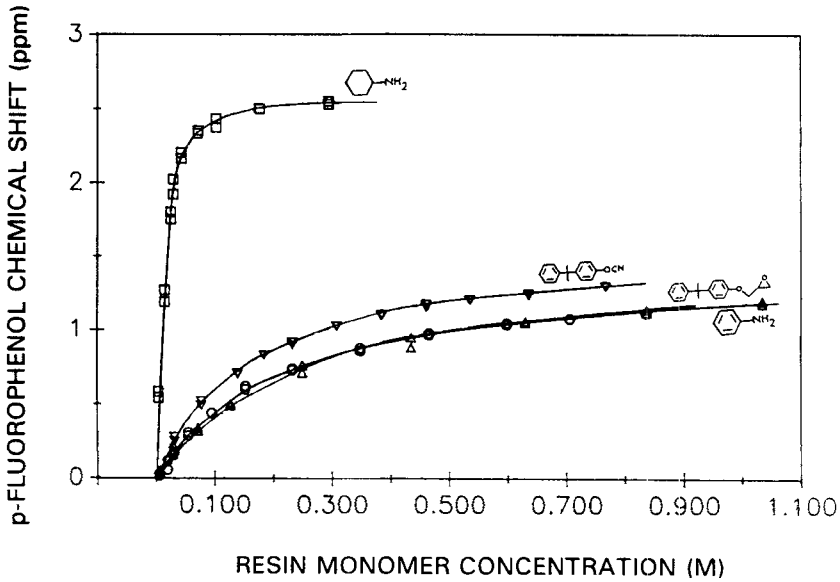

FIGURE 6 Resin monomer—*p*-fluorophenol hydrogen bond complexation data fit to equation (1) for determination of Δ and K_{HB} and calculation of β_Δ and β_K.

To place these β-scale hydrogen bond basicity measurements in perspective, literature values[27,28] from related compounds are reproduced in Table II. The β-scale ranges from 0 to 1 with hexamethylphosphotriamide as the strongest hydrogen bond acceptor base currently measured. The β-scale values for N,N-dimethtylaminocyclohexane and N,N-dimethyl-aniline are in good agreement with our measurements on the unmethylated analogues in Table I. No literature measurements were found for

TABLE II
β-Scale Hydrogen Bond Acceptor Strength Measurements of Relevant Compounds[27]

COMPOUND	β	COMPOUND	β
	.97		.41
	.71		.65
	.51		.47
	.39		

Downloaded At: 12:28 22 January 2011

cyanate or oxirane functionalized compounds. The measurement on cumylphenyl cyanate corresponds well with the literature measurement for benzonitrile. Literature tables of β-scale measurements also do not include triazine compounds, but extrapolation from the pyridine and pyrimidine heterocycle values appears to show consistency.

Comparison of monofunctional monomer and resin model compound β-scale basicities within the three resin systems indicates some interesting trends. In the cyanate resin system, the cyanurate polymer linkage structure is more basic than the cyanate functional group. While the cyanate resin system has no monomer stoichiometry to be upset by selective adsorption on a fiber surface, the stronger basicity of the cyanurate polymer linkage may have an effect on the curing reaction. This polymerization is catalyzed by Lewis bases,[29] and the stronger basicity of the cyanurate structure is a source of explanation for autocatalytic kinetics reported for cyanate polymerizations.[30]

Regarding the amine-epoxy resin systems, the large basicity difference between the aromatic and aliphatic amine monomers is reflected in the β-scale values. The aromatic amine basicity is low and is not significantly different from the glycidyl ether comonomer basicity. For this monomer pair, a stoichiometry mismatch caused by selective adsorption onto an acidic carbon fiber surface would not be expected. The corresponding resin model compound is a stronger hydrogen bond acceptor than either monomer and should be more strongly adsorbed onto the carbon fiber surface. For the aliphatic amine-epoxy system, there is a large difference in hydrogen acceptor strength between cyclohexyl amine and cumylphenylglycidyl ether, and the corresponding resin model compound has an intermediate β-scale value. In this case, the aliphatic amine monomer is predicted to have the strongest hydrogen bond association with the carbon fiber surface. The hydroxyl group in these amine-epoxy model compounds has a complicated role. It exercises an influence by its amphoteric character and by its intramolecular position relative to the amine group. As an independent functional group, the β-scale value of isopropanol (see Table II) could be considered representative of a secondary alcohol. In the aromatic amine-epoxy model compound, this functional group could be considered the most basic site making the increase in β-scale value relative to those of its monomers understandable. However, in the aliphatic amine-epoxy model compound, the aliphatic tertiary amine is the most basic site. It appears that the hydroxyl group has a levelling effect on the basicity of the aliphatic amine-epoxy model compound. As such, and intramolecular shielding is easily envisioned as illustrated by the structure below.

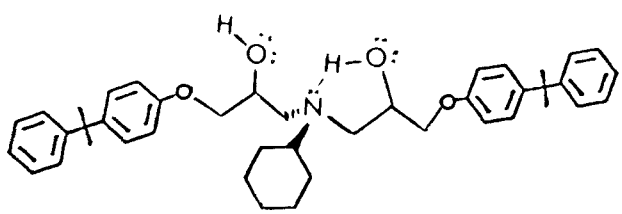

α-Scale Hydrogen Bond Donor Measurements

The hydrogen bond donor strength of the resin model compounds is measured by complex formation with a reference hydrogen bond acceptor compound. For this

Downloaded At: 12:28 22 January 2011

measurement, a UV spectroscopic method using pyridine N-oxide as the reference hydrogen bond acceptor compound was utilized.[14] This equilibrium for a 1:1 hydrogen bond complex with a hydroxyl group is illustrated below.

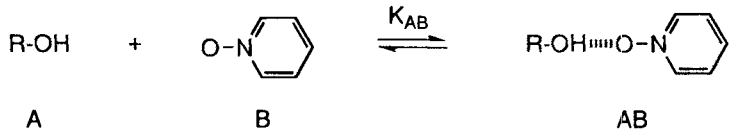

Pyridine oxide has two weak $n \rightarrow \pi^*$ absorptions in the near ultraviolet spectrum which are sensitive to hydrogen bonding.[31] When the oxygen-based nonbonded electron pair is committed to a hydrogen bond, the $n \rightarrow \pi^*$ absorption at 337.4 nm disappears. Thus, the intensity of this absorption becomes a measure of the free pyridine oxide concentration in a hydrogen bonded complex formation experiment. In this experiment, successive additions of the resin model compound are made to a dilute pyridine oxide/cyclohexane solution and the absorbance at 337.4 nm is measured. The pyridine oxide UV spectrum is illustrated in Figure 7 with the 337.4 nm absorbance decrease resulting from model compound addition depicted in the insert.

In choosing an equilibrium model to fit the data, the hydroxyl group causes complication because of its tendency to self associate. The amine-epoxy resin model compounds are further complicated by being dihydroxy compounds. The approach here is to start with the simplest equilibrium, test the fit of the data, observe trends between the resin model compounds and progress to more complicated models which require additional equilibrium steps.

Downloaded At: 12:28 22 January 2011

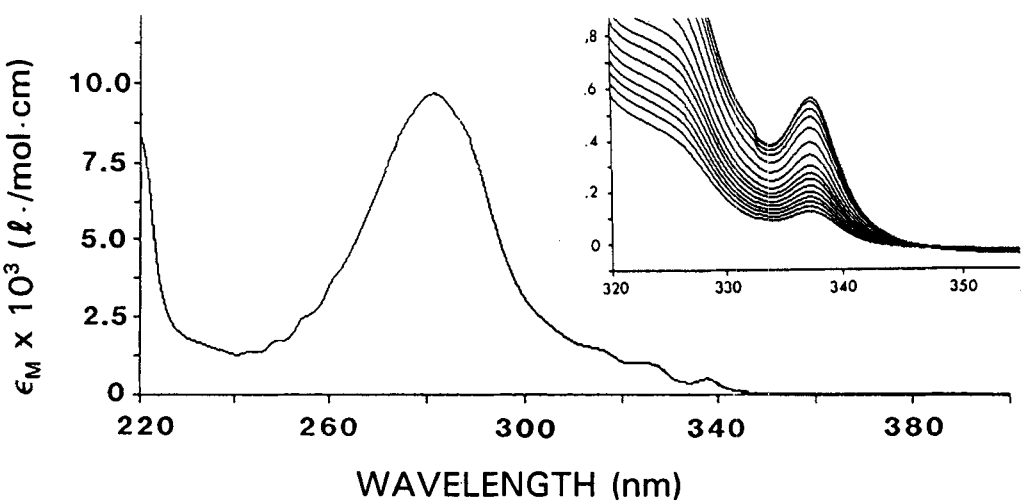

FIGURE 7 Electronic spectrum of pyridine N-oxide in cyclohexane solution. The insert illustrates the decreasing absorption of the 337.4 nm $n \rightarrow \pi^*$ transition caused by hydrogen bond complex formation with incremental additions of model compound.

The single-step equilibrium and expressions for determining the complex formation constant are depicted below where the subscripts A, B and AB represent the model compound, the pyridine oxide and the 1:1 hydrogen bonded complex, respectively, K_{AB} is the 1:1 complex formation constant, X and X^0 are the equilibrium and analytical mole fraction concentrations, and A^0 and A are the 337.4 nm absorbencies of the pyridine oxide/cyclohexane solution initially and subsequent to model compound addition, respectively.

$$K_{AB} = \frac{X_{AB}}{X_A X_B}$$

$$X_A^0 = X_A + X_{AB}$$

$$X_B^0 = X_B + X_{AB}$$

$$\frac{A^0}{A} = \frac{X_B^0}{X_B} \qquad A = \varepsilon b X_B$$

Combination of these expressions yields the following working equation to determine the equilibrium constant from the slope of a corresponding plot.

$$\frac{A^0 - A}{A} = K_{AB}\ [X_A^0 - (1 - (A/A^0))\ X_B^0] \tag{2}$$

For the situation where $X_{A^0} \gg X_{AB}$ (*i.e.* a weak equilibrium and/or high dilution conditions), the useful equivalent approximation of $X_{A^0} \gg (X_{B^0} - X_B)$ may be used to simplify equation (2) as follows.

$$\frac{A^0 - A}{A} = K_{AB}\ X_B^0 \tag{3}$$

The data for the three resin model compounds plotted according to equations (2) and (3) are presented in Figure 8. Also plotted in Figure 8 are data obtained using isopropanol as a relevant monofunctional compound. It is immediately apparent that there are large differences between these compounds. The cyanate resin model compound essentially forms no hydrogen bonded complex with the pyridine oxide as would be expected since it has no labile hydrogen to donate. The hydrogen bonded complex of the aliphatic amine-epoxy model compound is substantially weaker than that of the aromatic amine-epoxy model compound. Data for these two compounds are plotted both with the $X_{A^0} \gg (X_{B^0} - X_B)$ approximation (filled symbols, equation (3)) and without this approximation (open symbols, equation (2)). As expected, the approximation is closer to the exact solution for the weaker complex, but the close coincidence in two cases justifies use of the approximation which is necessary in more complicated equilibrium models. The isopropanol data were taken to demonstrate differences

Downloaded At: 12:28 22 January 2011

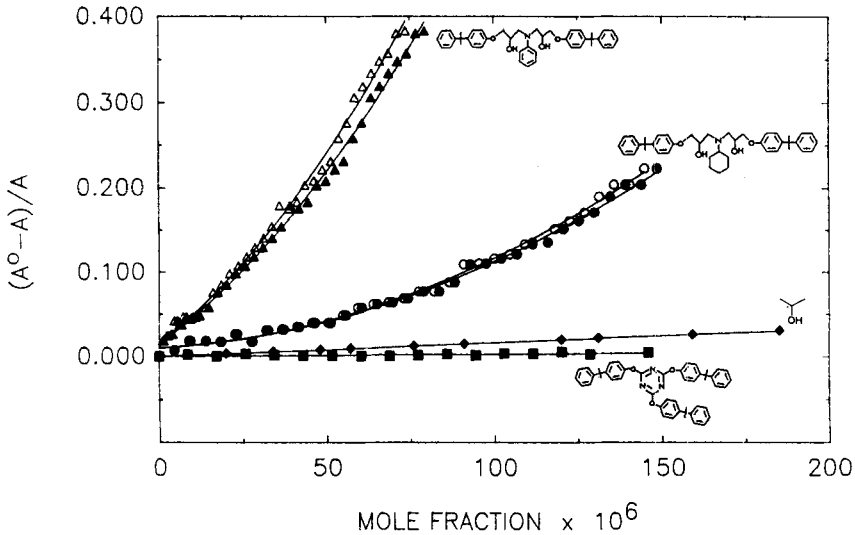

FIGURE 8 Resin model compound—pyridine N-oxide hydrogen bond complexation data plotted for the single-step equilibrium model according to equation (2) (open symbols) and equation (3) (filled symbols). Data for isopropanol are also included.

Downloaded At: 12:28 22 January 2011

between a simple monofunctional compound and the polyfunctional model compounds of this study. While isopropanol has the same secondary alcohol structure of the amine-epoxy compounds, it is a much weaker hydrogen bond donor. *This observation demonstrates that hydrogen bond strengths of polyfunctional molecular structures cannot be assessed on the basis of isolated functional groups.* If this single- step equilibrium model completely represented the hydrogen bonded complex behavior, the plot would be linear-which it is not. If the initial portion of the plot is considered to be linear, complex formation constants may be calculated from the initial slopes. These constants are entered in Table III for the amine-epoxy compounds.

An obvious extension of the one step equilibrium model is a two step equilibrium model where each hydroxyl group is sequentially complexed with a pyridine oxide molecule.

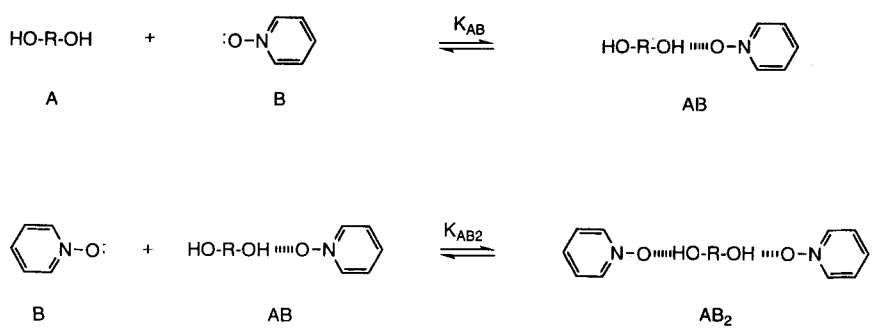

In this case there are two complex formation constants. To test this model a linear equation relating the 337.4 nm pyridine oxide absorbance and the epoxy adduct and pyridine oxide mole fractions may be derived. The expressions from which equation (2) is derived are utilized along with the $X_{A^\circ} \gg (X_{B^\circ} - X_B)$ approximation. When this is done, the following equation is obtained.

$$\frac{A^0 - A}{A} \frac{1}{X_A^0} = -2 K_{AB} K_{AB2} X_B^0 \left(\frac{A}{A^0}\right) + K_{AB} \tag{4}$$

The data for the two amine-epoxy model compounds plotted according to equation (4) are presented in Figure 9. This plot shows again that the aromatic amine epoxy is the stronger hydrogen bond donor. The scatter as A/A^0 approaches 1 results from measurement difficulties as both $(A^0 - A)$ and X_{A° become small. Lower values of A/A^0 were not obtainable because of solubility limits of the amine epoxy model compounds in cyclohexane. The plot does deviate from linearity, indicating that the two-step equilibrium model is not rigorously followed. Using the linear portion of the plot indicated, complex formation constants have been calculated from the slopes and intercepts and are entered in Table III. In a semiquantitative fashion these constants do highlight the differences between these compounds. Also, the apparent hydrogen bond donor strength of the second hydroxyl group is much increased by the hydrogen bonding of the first.

It has been demonstrated that self-association of alcohols (*i.e.* dimerization) has an enhancing effect on hydrogen bond acidity.[14] This consideration requires a three-step equilibrium model.

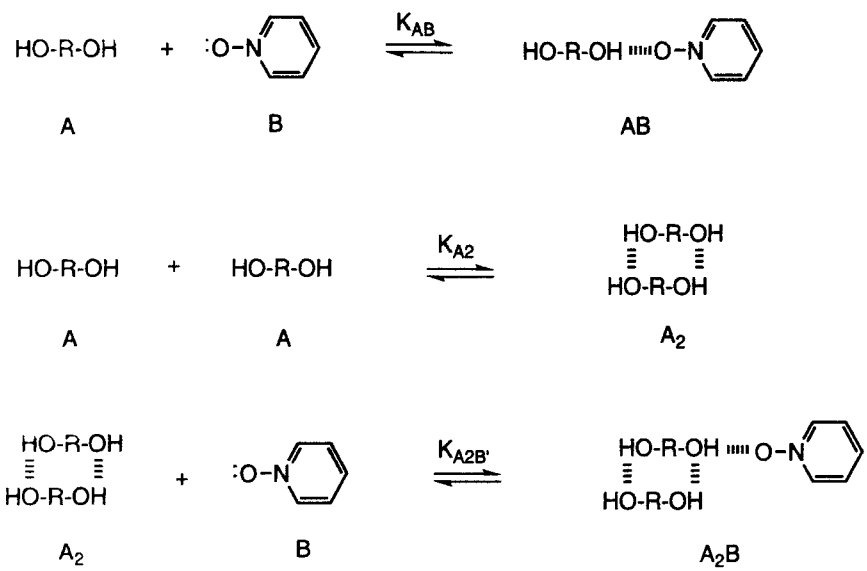

Downloaded At: 12:28 22 January 2011

It is not possible to reduce this model to a linear working equation. A methodology for data handling of this model has been reported,[14] as referred to in the Experimental Section. The corresponding constants for the three equilibria are presented in Table III. The constant for the formation of the 1:1 model compound:pyridine oxide complex, K_{AB}, is similar to that for the one-step equilibrium model. The intermolecular self-association constant, K_{A2}, is much smaller than K_{AB}. The constant for associated dimer complexed with pyridine oxide, $K_{AB'}$, is much greater than that for the unassociated alcohol which is consistent with the previously-reported trend.[14] If the second step in this three-step model is modified so that it is an intramolecular association of hydroxyl groups instead of an intermolecular association, as illustrated below, a linear working equation using the $X_{A^0} \gg (X_{B^0} - X_B)$ approximation is derived.

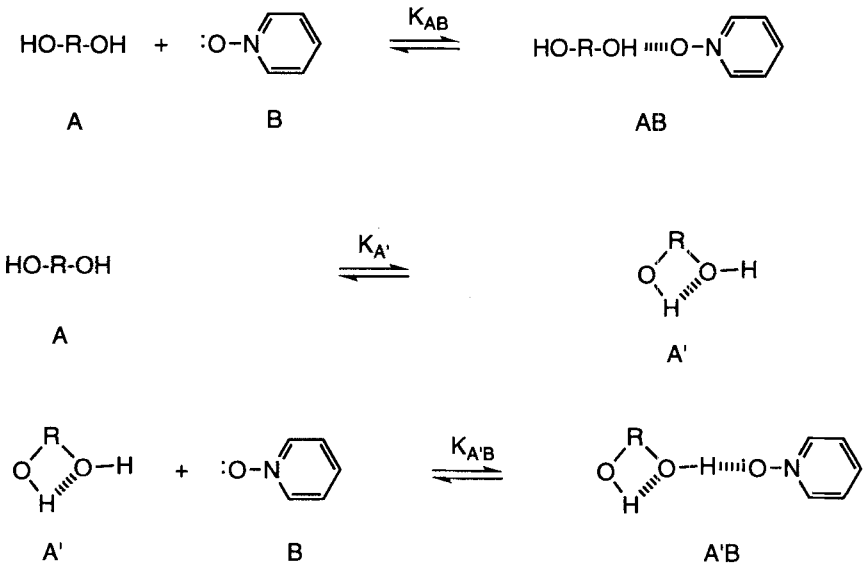

$$\frac{A^0 - A}{A} = \frac{K_{AB} + K_{A'}K_{A'B}}{K_{A'} + 1} X_A^0$$

This equation has the same linear form as that for the one-step equilibrium model, but its slope is proportional to a function of the three equilibrium constants. These are not individually solvable.

Regardless of which equilibrium model is used, the result is the same. The three resin model compounds differ substantially in strength of hydrogen bond complex formation. The order is aromatic amine-epoxy > aliphatic amine-epoxy ≫ cyanate.

A α-scale of hydrogen bond donor strength has been defined which is independent of the hydrogen bond acceptor reference compound and is normalized to a scale of 0 to 1.[14c] The respective α-scale correlation equation for the pyridine N-oxide reference compound K_{AB} values (in molarity units) is:[14c]

$$\alpha = 0.069 + 0.185 \log K_{AB}$$

Downloaded At: 12:28 22 January 2011

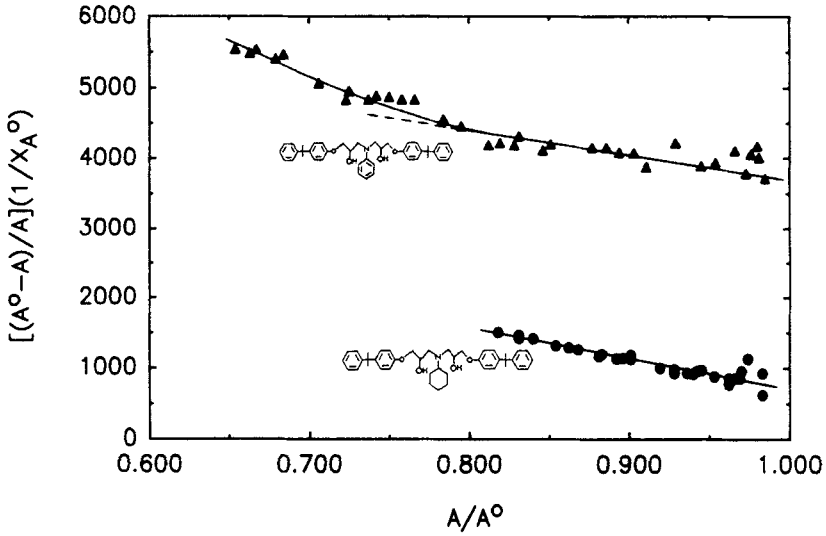

FIGURE 9 Amine-epoxy model compound—pyridine N-oxide hydrogen bond complexation data plotted for the two-step equilibrium model according to equation (4).

Downloaded At: 12:28 22 January 2011

The α-scale values for the three resin model compounds based on K_{AB} values from the single-step model are entered in Table IV. For comparison, some literature α-scale values of relevant monofunctional compounds are also entered in Table IV. For the purpose of direct comparison with the literature, data are also collected for 2-propanol. These data are plotted in Figure 8. It is immediately evident from Figure 8 and Table IV that both epoxy-amine model compounds are significantly stronger hydrogen bond donors than 2-propanol and are approaching the donor strength of very acidic alcohols. As to why the aliphatic amine-epoxy compound is a weaker hydrogen bond donor than the aromatic amine-epoxy compound, it appears that an intramolecular interaction between both hydroxyls and the amine site as sketched below may provide an explanation.

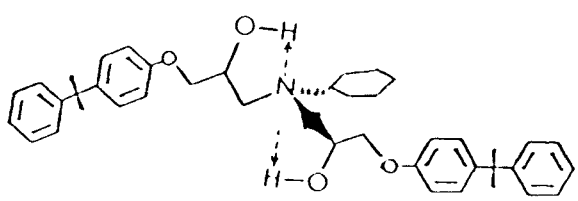

Speculation is that the more basic aliphatic amine ties up both hydroxyl groups by way of a rapid pyramidal inversion with a stronger intramolecular hydrogen bonded interaction resulting in a weaker intermolecular hydrogen bond with competing bases.

TABLE III
Pyridine N-Oxide-Amine-Epoxy Model Compound Hydrogen Bond Complex Formation Constants (mole fraction units) for One, Two and Three Step Equilibrium Models.

One Step

$$A + B \underset{}{\overset{K_{AB}}{\rightleftharpoons}} AB$$

	K_{AB}
Aliphatic Amine Epoxy	1000
Aromatic Amine Epoxy	4300

Two Step

$$A + B \overset{K_{AB}}{\rightleftharpoons} AB$$

$$AB + B \overset{K_{AB2}}{\rightleftharpoons} AB_2$$

	K_{AB}	K_{AB2}
Aliphatic Amine Epoxy	5200	21,000
Aromatic Amine Epoxy	10,500	17,000

Three Step

$$A + B \overset{K_{AB}}{\rightleftharpoons} AB$$

$$A + A \overset{K_{A2}}{\rightleftharpoons} A_2$$

$$A_2 + A \overset{K_{A2B}}{\rightleftharpoons} A_2B$$

	K_{AB}	K_{A2}	K_{A2B}
Aliphatic Amine Epoxy	720	.005	1.0×10^7
Aromatic Amine Epoxy	3500	.011	2.1×10^7

Downloaded At: 12:28 22 January 2011

Resin-Fiber Interface Load Transfer

As a diagnostic of resin-fiber interfacial adhesion, the single fiber fragmentation test was used to measure the interfacial shear strength.[32] In this test a single AS4 carbon fiber is encapsulated along the axis of a dogbone-shaped resin sample. As the specimen is strained, the fiber is fragmented due to load transfer from a shear stress of the resin across the interface to a tensile stress on the fiber. With continued strain, fragmentation of the fiber continues until a critical fragment length is reached. At this point the fiber

TABLE IV
α-Scale Hydrogen Bond Donor Strength Measurements on Amine-Epoxy and Cyanate Resin Model Compounds and Literature Reference Compounds.[14]

Model Compound	α
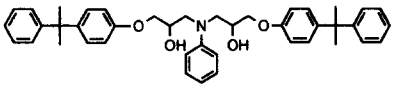	0.56
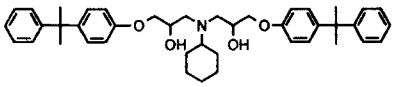	0.44
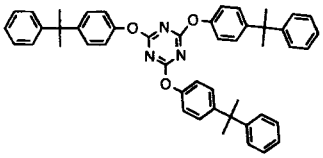	0
Reference Compound	
Cl_3CH	0.18
	0.30
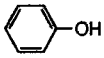	0.63
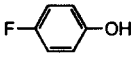	0.69
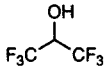	0.78

fragment length no longer presents sufficient surface area for the load transfer to exceed the fiber tensile strength. The interfacial shear strength (τ_c) is calculated from an inverse relationship with the critical fiber fragment length:

$$\tau_c = \frac{\sigma_c d}{2 l_c}$$

where l_c is the fiber fragment critical length below which stress transfer from the resin is insufficient for further fiber breakage, σ_c is the fiber tensile strength (at l_c gauge length)

Downloaded At: 12:28 22 January 2011

and d is the fiber diameter. Since the distribution of the measured fragment lengths ranges from $1/2 l_c$ to l_c, the value of l_c has been approximated by $(4/3)\, l_f$ where l_f is the average measured fragment length.[33]

This test requires that the resin strain-to-break exceed that of the fiber by at least a factor of 3 to 4 in order to reach the critical fiber length before the resin fails. The AS4 fiber failure strain is approximately 1 percent, thus the resin strain-to-break should be greater than 3 to 4 percent. The cyanate resin, when cured with a conventional cool down after cure, does not meet this criterion. However, it was discovered, in a physical aging study, that a rapid thermal quenching of the aromatic amine-epoxy resin resulted in a significant increase in tensile strain-to-break while having no effect on the critical length[25] in the single fiber fragmentation test. Tensile tests were conducted on the amine-epoxy and cyanate resins which were cooled slowly as well as rapidly quenched from above the glass transition temperature to quantify this effect on these properties. The results of this testing of the three resin systems are presented in Table V. In each case, the quenched resin is more ductile than the slowly-cooled resin. For the cyanate resin, the 0.4% increase in strain-to-break is sufficient to allow straining to the AS4 fiber critical fragment length before failure of the test specimen. For the epoxy resins, the strain-to-break increase is 1 to 2%. The mechanical property differences between the two epoxy resins are very small, consistent with the design of this experiment so that these resins have minimal structure and property variation except for hydrogen bond strengths. The initial modulii of the three resins are remarkably similar.

The single fiber fragmentation test results for the aromatic amine-epoxy, cyanate and aliphatic amine-epoxy are presented in Table VI along with the hydrogen bond acceptor and donor strength parameters for the resins. The resins are listed in the order of decreasing interfacial shear strengths. The interfacial shear strengths of the resins

Downloaded At: 12:28 22 January 2011

TABLE V
Tensile Mechanical Properties of Amine-Epoxy and Cyanate Resins with Slow-Cooled and Quenched Thermal Histories.

Resin	Break Strain (%)	Initial Modulus (MPA)	Break Stress (MPA)	Tg (°C)
Aromatic Amine Epoxy				
Slow-Cooled	5.3	3000 ± 80	87 ± 3.0	166
Quenched	7.4	2970 ± 110	89	
Aliphatic Amine Epoxy				
Slow-Cooled	5.8 ± 1.1	2990 ± 40	91 ± 5.3	146
Quenched	6.7 ± 0.8	3010 ± 180	88 ± 1.9	
Bisphenol A Dicyanate				
Slow-Cooled	3.3 ± 0.2	3200 ± 110	87 ± 5.4	280
Quenched	3.7 ± 0.3	3070 ± 30	90 ± 6.4	

TABLE VI
AS4 Single Fiber Critical Length Test Results and Hydrogen Bond Acceptor and Donor Strengths.

Resin	ℓ_f (mm)	τ_c[a] (MPA)	β	α
Aromatic Amine Epoxy	0.40	40	0.43	0.56
Bisphenol A Dicyanate	0.34	49	0.48	0
Aliphatic Amine Epoxy	0.31	54	0.51	0.44

a; Calculated from AS4 fiber data[15]: d = 7.1 μ; $\ln \sigma_c = -0.179 \ln \ell_c + 3.0833$; σ_c(grams), ℓ_c(mm).

with the AS4 fiber increase in the order MPDA-epoxy < cyanate < DACH-epoxy. The AS4-epoxy system has previously been characterized by the fragmentation test as an example of "good adhesion".[32] By correlation of interfacial shear strength with adhesion, the cyanate and DACH-epoxy resins are also characterized by good adhesion to the AS4 fiber. Associated with "good adhesion" is an intense and uniform birefringent pattern that develops around the fiber as the test is performed.[32] This is observed for the resins of this work. As shown in Table VI and in Figure 10, there is a good correlation between the interfacial shear strength and the resin β-scale hydrogen

Downloaded At: 12:28 22 January 2011

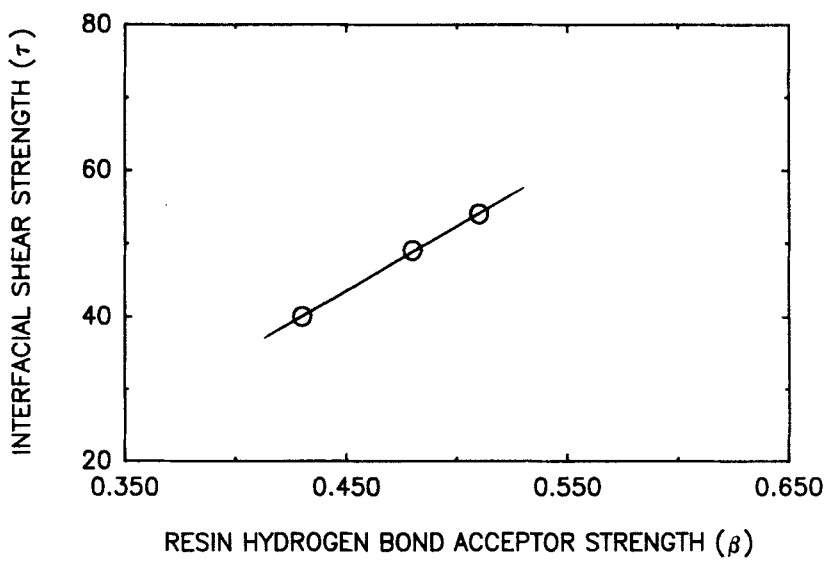

FIGURE 10 Correlation plot of resin β-scale hydrogen bond acceptor strength *vs.* single fiber-resin interfacial shear strength for the MPDA-epoxy, DACH-epoxy and cyanate resins with the AS4 carbon fiber.

bond acceptor strength. This reflects the acidic character of the AS4 fiber surface interacting with the basic nature of the resin structure. There is no correlation with the α-scale hydrogen bond donor strength indicating the acidic nature of the resin structure is unimportant. The range of these data is confined to τ values (40 to 54 MPA) indicative of good adhesion and to β-scale values (0.43 to 0.51) indicative of moderately-high hydrogen bond acceptor strength. These ranges are significant and practical in the sense that they coincide with that desirable and found in useful composites and resins.

Control of resin structure can result in meaningful variation of fiber-resin adhesion by hydrogen bonded interaction. This statement assumes that the mechanical property contribution of the resin to the interfacial shear strength measurement is an invariant factor. Consideration of this assumption is a factor in the selection of resins for this study, and the consequent mechanical property data of Table V are in support of this assumption. Variation in matrix mechanical properties has been reported to influence the fiber fragmentation test results,[34] and the design in this experiment is to eliminate or minimize this effect. This work indicates that matrix resin hydrogen bonded interactions can significantly contribute to fiber interface adhesion. While quantitative measurement and understanding of the hydrogen bonded interaction is complicated by the polyfunctional character of the resin structure, incorporation of hydrogen bonding sites into the resin structure is an option for enhancement and control of interfacial adhesion.

Downloaded At: 12:28 22 January 2011

SUMMARY

A spectroscopic method based on using model compounds to measure and rank thermoset resin hydrogen bond acceptor and donor strengths is demonstrated. This involves measurements of hydrogen bonded complex formation constants between polyfunctional resin model compounds and monofunctional probe compounds. For the epoxy and cyanate resins in this study, the ranking of hydrogen bond basicity is aliphatic amine-epoxy > cyanate > aromatic amine-epoxy, and the ranking of hydrogen bond acidity is aromatic amine-epoxy > aliphatic amine-epoxy ≫ cyanate. For the amine-epoxy resin model compounds, intramolecular interactions between the amine and hydroxyl groups reduce the hydrogen bond acceptor strength and enhance the hydrogen bond donor strength, relative to expectations for these individual functional groups acting independently.

Measurements of the hydrogen bond basicity of the resin monomer model compounds have also been made. These measurements on the amine and epoxy monomers indicate there is little basis for a hydrogen bonded selective adsorption of the aromatic amine on to a carbon fiber surface relative to the epoxy monomer. The aliphatic amine is substantially more basic than the epoxy, and selective adsorption and stoichiometry alteration driven by hydrogen bonding at the carbon fiber surface may occur. The cyanate resin monomer is less basic than the cyanurate polymer linkage. While there is no monomer stoichiometry to be affected by selective adsorption at the fiber interface, the stronger cyanurate basicity may be a factor in the autoacceleration of the curing reaction.

Interfacial shear strength measurements on quenched single fiber epoxy and cyanate fragmentation test specimens are indicative of good adhesion and displayed a depend-

ence on resin structure. The order of increasing adhesion for the matrix resin with the AS4 carbon fiber is MPDA-epoxy < cyanate < DACH-epoxy. This order parallels that of the β-scale hydrogen bond acceptor strength. Variation in the resin mechanical properties is minimal, and a hydrogen bonding mechanism is proposed to account for the correlation of fiber- matrix interfacial shear strength and resin hydrogen bond acceptor strength.

Acknowledgement

The authors gratefully acknowledge D. A. Shimp of Ciba-Geigy, for helpful discussion and arranging contribution of the bisphenol A dicyanate. Dr. W. R. Barger of NRL is gratefully acknowledged for development of iteration computer programs necessary for equilibrium constant determination. This work was supported by the Office of Naval Research.

References

1. A. Garton, S. Wang and W. T. K. Stevenson, in *Composite Applications: The Role of Matrix, Fiber, and Interface*, T. Vigo and B. Kinzig, Eds. (VCH Publishers, New York, 1992), Chapt. 11.
2. J. Schultz and L. Lavielle, in *Inverse Gas Chromatography, Characterization of Polymers and Other Materials*, D. R. Lloyd, T. C. Ward, H. P. Schreiber and C. C. Pizaña, Eds., ACS Symp. Ser. **391** (American Chemical Society, Washington, D. C., 1989), Chapt. 14; J. Schultz, L. Lavielle and C. Martin, *J. Adhesion* **23**, 45 (1987).
3. W. Gordy, *J. Am. Chem. Soc.* **60**, 605 (1938).
4. G. C. Pimentel and A. L. McClellan, *The Hydrogen Bond* (W. H. Freeman and Company, San Francisco, 1960).
5. R. M. Badger and S. H. Bauer, *J. Chem. Phys.* **5**, 839 (1937); R. M. Badger, *J. Chem. Phys.* **8**, 288 (1940).
6. M. D. Joesten and R. S. Drago, *J. Am. Chem. Soc.* **84**, 3817 (1962).
7. M. J. Kamlet, R. R. Minesinger and W. H. Gilligan, *J. Am. Chem. Soc.* **94**, 4744 (1972).
8. V. Gutmann, *The Donor-Acceptor Approach to Molecular Interactions* (Plenum Press, New York, 1983).
9. (a) M. J. Kamlet and R. W. Taft, *J. Am. Chem. Soc.* **98**, 377 (1976); (b) R. W. Taft and M. J. Kamlet, *J. Am. Chem. Soc.* **98**, 2886 (1976).
10. M. H. Abraham, *Chem. Soc. Rev.* **22**, 73 (1993).
11. J. F. Watts and M. M. Chehimi, *J. Adhesion* **41**, 81 (1993).
12. F. M. Fowkes, D. W. Dwight and D. A. Cole, *J. Non-Cryst. Solids* **120**, 47 (1990).
13. D. Gurka and R. W. Taft, *J. Am. Chem. Soc*, **91**, 4794 (1969).
14. (a) B. Frange, J. L. Abboud, L. Bellon and C. Bénamou, *Bull. Soc. Chim. France* **1**, 134 (1982); (b) B. Frange, J. L. Abboud, L. Bellon and C. Bénamou, *J. Org. Chem.* **47**, 4553 (1982); (c) J. L. Abboud, K. Sraidi, M. H. Abraham and R. W. Taft, *J. Org. Chem.* **55**, 2230 (1990).
15. J. P. Armistead and A. W. Snow, *Polymer Composites* **15**, 385 (1994).
16. J. P. Armistead, A. W. Snow and W. D. Bascom, *19th International SAMPE Technical Conference Proceedings*, Vol. 19, 644 (1987).
17. W. W. Wright, *Composite Polymers* **3** (4), 231 (1990).
18. B. -W. Chun, C. R. Davis, Q. He and R. R. Gustafson, *Carbon* **30**, 177 (1992).
19. C. A. Baille, J. F. Watts and J. E. Castle, *J. Mater. Chem.* **2** (9), 939 (1992).
20. K. Morita, Y. Murata, A. Ishitani, K. Murayama, T. Ono and A. Nakajima, *Pure & Appl. Chem.* **58**, 455 (1986).
21. J. -B. Donnet and R. C. Bansal, *Carbon Fibers*, 2nd ed. (Marcel Dekker, Inc., New York, 1990).
22. R. Yosomiya, K. Morimoto, A. Nakajima, Y. Ikada and T. Suzuki, *Adhesion and Bonding in Composites* (Marcel Dekker, Inc., New York, 1990) Chapt. 10.
23. R. F. Cozzens, P. Walter and A. W. Snow, *J. Appl. Polym. Sci.* **34**, 601 (1987).
24. D. A. Shimp, US Patent 4, 847, 233 (1989).
25. J. P. Armistead and A. W. Snow, *J. Adhesion*, this issue.
26. M. L. Kaplan, M. L. Schilling and A. M. Mujsce, *J. Polym. Sci.* **A29**, 599 (1991).
27. M. J. Kamlet, J. L. Abboud, M. H. Abraham and R. W. Taft, *J. Org. Chem.* **48**, 2877 (1983).
28. J. L. Abboud, K. Sraidi, G. Guiheneuf, A. Negro, M. J. Kamlet and R. W. Taft, *J. Org. Chem.* **50**, 2870 (1985); M. J. Kamlet, R. M. Doherty, J. M. Abboud, M. H. Abraham and R. W. Taft, *Chemtech* **16**, 566 (1986).

Downloaded At: 12:28 22 January 2011

29. E. Grigat and R. Pütter, *Chem. Ber.* **97,** 3012 (1964).
30. S. L. Simon and J. K. Gillham, *J. Appl. Polym. Sci.* **47,** 461 (1993).
31. M. Ito and N. Hata, *Bull. Chem. Soc. Japan* **28,** 260 (1955).
32. (a) L. T. Drzal, M. J. Rich and P. F. Lloyd, *J. Adhesion* **16,** 1 (1982); (b) W. D. Bascom and R. M. Jensen, *J. Adhesion* **19,** 219 (1986).
33. A. S. Wilmolkiatisak and J. P. Bell, *Polymer Composites* **10,** 162 (1989).
34. L. T. Drzal, *Mat. Sci. Eng.* **A126,** 289 (1990).

Downloaded At: 12:28 22 January 2011